Protein Science (1998), 7:243–253. Cambridge University Press. Printed in the USA.

Hirunorms are true hirudin mimetics. The crystal structure of human α-thrombin–hirunorm V complex

GIUSEPPINA DE SIMONE,[1] ANGELA LOMBARDI,[1] STEFANIA GALDIERO,[1] FLAVIA NASTRI,[1] ROSSELLA DELLA MORTE,[2] NORMA STAIANO,[2] CARLO PEDONE,[1] MARTINO BOLOGNESI,[3,4] AND VINCENZO PAVONE[1]

[1]Centro Interuniversitario di Ricerca su Peptidi Bioattivi, & Centro di Studio di Biocristallografia—CNR, University of Napoli "Federico II," via Mezzocannone 4, 80134 Napoli, Italy
[2]Dipartimento di Biochimica e Biotecnologie Mediche, University of Napoli "Federico II," via Pansini 5, 80129 Napoli, Italy
[3]Dipartimento di Genetica e Microbiologia, University of Pavia, Via Abbiategrasso 207, 27100 Pavia, Italy
[4]Advanced Biotechnology Center and Department of Physics, University of Genova, Largo Rosanna Benzi, 10, 16132 Genova, Italy

(RECEIVED July 31, 1997; ACCEPTED October 22, 1997)

Abstract

A novel class of synthetic, multisite-directed thrombin inhibitors, known as hirunorms, has been described recently. These compounds were designed to mimic the binding mode of hirudin, and they have been proven to be very strong and selective thrombin inhibitors. Here we report the crystal structure of the complex formed by human α-thrombin and hirunorm V, a 26-residue polypeptide containing non-natural amino acids, determined at 2.1 Å resolution and refined to an *R*-factor of 0.176. The structure reveals that the inhibitor binding mode is distinctive of a true hirudin mimetic, and it highlights the molecular basis of the high inhibitory potency (K_i is in the picomolar range) and the strong selectivity of hirunorm V.

Hirunorm V interacts through the N-terminal tetrapeptide with the thrombin active site in a nonsubstrate mode; at the same time, this inhibitor specifically binds through the C-terminal segment to the fibrinogen recognition exosite. The backbone of the N-terminal tetrapeptide Chg$^{1''}$–Val$^{2''}$–2-Nal$^{3''}$–Thr$^{4''}$ (Chg, cyclohexyl-glycine; 2-Nal, β-(2-naphthyl)-alanine) forms a short β-strand parallel to thrombin main-chain residues Ser^{214}–Gly^{219}. The Chg$^{1''}$ side chain fills the S2 subsite, Val$^{2''}$ is located at the entrance of S1, whereas 2-Nal$^{3''}$ side chain occupies the aryl-binding site. Such backbone orientation is very close to that observed for the N-terminal residues of hirudin, and it is similar to that of the synthetic retro-binding peptide BMS-183507, but it is opposite to the proposed binding mode of fibrinogen and of small synthetic substrates. Hirunorm V C-terminal segment binds to the fibrinogen recognition exosite, similarly to what observed for hirudin C-terminal tail and related compounds. The linker polypeptide segment connecting hirunorm V N- and C-terminal regions is not observable in the electron density maps. The crystallographic analysis proves the correctness of the design and it provides a compelling proof on the interaction mechanism for this novel class of high potency multisite-directed synthetic thrombin inhibitors.

Keywords: antithrombotics; hirudin-like binding mode; hirunorms; thrombin; thrombin synthetic inhibitors; X-ray crystal structure

Reprint requests to: Vincenzo Pavone, Centro Interuniversitario di Ricerca su Peptidi Bioattivi, via Mezzocannone 4, 80134 Napoli, Italy; e-mail: pavone@chemna.dichi.unina.it.

Abbreviations: thrombin, human α-thrombin; PPACK, D-Phe-Pro-Arg chloromethylketone; FPAM, fibrinopeptide A mimetic; NAPAP, N$^{\alpha}$-(2napthylsulphonyl-glycyl)-DL-*p*-amidinophenylalanyl-piperidine; MQPA, (2R,4R)-4-methyl-1-[N$^{\alpha}$-((RS)-3-methyl-1,2,3,4-tetrahydro-8-quinolenesulphonyl)-L-arginyl]-2-piperidine carboxylic acid; 4-TAPAP, N$^{\alpha}$-(4-toluene-sulphonyl)-DL-*p*-amidino phenylalanyl-piperidine; 3-TAPAP, N$^{\alpha}$-(4-toluene-sulphonyl)-DL-*m*-amidino phenylalanyl-piperidine; BMS-186282, [S-(R*,R*)]-[4-(aminoiminomethyl)-amino]-*N*-[[1-[3-hydroxy-2-[(2-naphthalenylsulfonyl)amino]-1-oxopropyl]-2-pyrrolidinyl]methyl]butanamide; BMS-189090 [S-(R*,R*)]-[1-(aminoiminomethyl)-amino]-*N*-[[1-[3-hydroxy-2-[(2-*n*aphthalenylsulfonyl) amino]-1-oxopropyl]-2-pyrrolidinyl]methyl]butanamide; BMS-183507, *N*-[*N*-[*N*-[4-(aminoiminomethyl)-amino]-1-oxobutyl]-L-phenylalanyl]-L-*allo*-threonyl]-L-phenylalanine methyl ester; Dmc-azalys, N$^{\alpha}$-(*N*,*N*-dimethylcarbamoyl)-α-azalysine; tPa, human tissue plasminogen activator; Chg, cyclohexyl-glycine; 2-Nal, β-(2-naphthyl)-alanine; h-Phe, (+)-α-amino-4-phenylbutyric acid; Aib, α-aminoisobutyric acid; Cha, β-cyclohexyl-alanine; residue numbering is primed in hirudin and double primed in hirunorm V, respectively; S1, S2, and S3 are the active site proteinase subsites, defined according to Schechter and Berger (1967).

Thrombin (EC 3.4.21.5) is a trypsin-like serine proteinase that participates as a primary enzyme in promoting coagulation (Fenton & Bing, 1986; Berliner, 1992; Stubbs & Bode, 1993). It is responsible for catalyzing the conversion of fibrinogen to fibrin (Fenton, 1986; Fenton et al., 1988, 1991) and it is the most potent stimulator of platelet aggregation (Tollefsen et al., 1974). It also activates blood coagulation factors V, VIII, which are essential for blood coagulation (Davie et al., 1991). Cardiovascular diseases are related to anomalies in the coagulation processes, leading to blockage of coronary arteries by thrombi; therefore, many efforts have been devoted in recent years to the development of human α-thrombin inhibitors as antithrombotics. Several natural and synthetic thrombin inhibitors have been studied in detail and characterized at atomic resolution in their interaction with thrombin (Berliner, 1992; Stubbs & Bode, 1993; Tulinsky & Qui, 1993). These studies bear a fundamental value for computer-assisted rational design of novel thrombin inhibitors with improved pharmacological properties, and they also shed light on novel aspects of molecular recognition, which may be broader than predictable (Salemme et al., 1997).

Thrombin inhibitors bind to their target enzyme by different interaction mechanisms, as schematically depicted in Figure 1.

1. Active site-directed peptidic or peptide-related inhibitors may interact with the active site (like fibrinogen in Fig. 1A) in a substrate mode, as commonly observed in serine proteinases of the same homology family (Bode & Huber, 1992; Laskowski & Kato, 1980). They align their backbone antiparallel to thrombin segment Ser^{214}–Glu^{217} (Fig. 1B). The peptide-based inhibitors cyclotheonamide (Maryanoff et al., 1993), PPACK (Bode et al., 1989, 1992b; Banner & Hadvary, 1991; Priestle et al., 1993), FPAM (Nakanashi et al., 1992; Wu et al., 1993) and the nonpeptide inhibitors MQPA (also called MD805; Okamoto et al., 1981; Kikumoto et al., 1984), NAPAP, 4-TAPAP, 3-TAPAP (Stürzebecher et al., 1983, 1984; Banner & Hadvary, 1991; Brandstetter et al., 1992), BMS-186282, and BMS-189090 (Malley et al., 1996) interact with thrombin by the use of this particular mechanism.
2. Active site-directed peptidic inhibitors may also interact in a nonsubstrate mode. They align the peptide backbone parallel to thrombin segment Ser^{214}–Glu^{217} (Fig. 1C). BMS-183507 (Iwanowicz et al., 1994; Tabernero et al., 1995) is an example.
3. Fibrinogen recognition exosite (FRE)-directed inhibitors, such as hirugen and hirugen-related peptides (Krstenansky & Mao, 1987; Krstenansky et al., 1987, 1988; Jakubowski & Maraganore, 1990; Skrzypczak-Jankun et al., 1991), hirudin$^{54-65}$ (Banner & Hadvary, 1991; Stubbs et al., 1992; Priestle et al., 1993), hirullin$^{50-62}$ (Krstenansky et al., 1990b; Qiu et al., 1993), thrombin receptor$^{49-61}$ (Vu et al., 1991; Mathews et al., 1994), and MD-6 (also called MDL-28,050; Krstenansky et al., 1990a), interact with thrombin in a canyon of the thrombin surface, which is apart from the catalytic site (Fig. 1D).
4. Multisite-directed inhibitors bind both to the catalytic site in an antiparallel fashion and to the FRE (Fig. 1E): hirulogs (Maraganore et al., 1990; Skrzypczak-Jankun et al., 1991; Qiu et al., 1992), hirulog derivatives (Krishnan et al., 1996), hirutonins (Szewczuk et al., 1993; Zdanov et al., 1993), P498 and P500 (Tsuda et al., 1994; Féthière et al., 1996) are examples of this class.
5. Hirudin, which is unique for its mutiple binding, interacts with the catalytic site in a nonsubstrate mode (i.e., with the N-terminal tail parallel to thrombin segment Ser^{214}–Glu^{217}), and it is also bound to the FRE (Fig. 1F) (Stone & Hofsteenge, 1986; Grütter et al., 1990; Rydel et al., 1990, 1991; Markwardt, 1994).

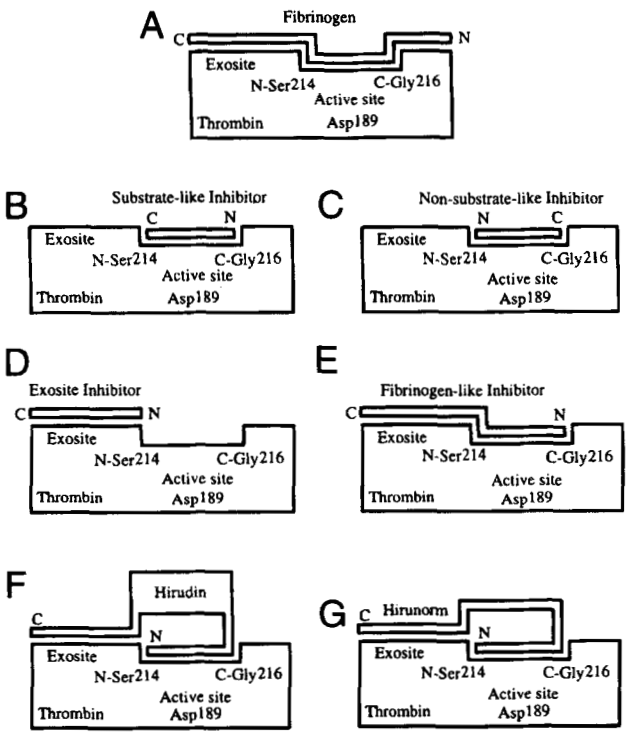

Fig. 1. Schematic representation of different interaction mechanisms between thrombin inhibitors and thrombin.

From this particular view point on the different mechanism of action, the synthetic inhibitors hirulogs (Maraganore et al., 1990) and hirutonins (Szewczuk et al., 1993) should be considered more precisely as fibrinogen-related peptides, even though they were derived originally from a knowledge-based approach, considering the thrombin–hirudin interaction (Grütter et al., 1990). They actually bind to thrombin similarly to fibrinogen, and differently from hirudin in the active site region. The peculiar binding mode of hirulog 1, as for fibrinogen itself, is the structural basis for its catalytic cleavage by thrombin. Hirulog variants, bearing noncleavable peptide bond surrogates, were thus developed, to abolish the suicide phenomena of binding, inhibition, and hydrolysis (DiMaio et al., 1991, 1992; Kline et al., 1991; Qiu et al., 1992; Krishnan et al., 1996).

Hirunorm V, a synthetic polypeptide composed of 26 residues (see Table 1; Lombardi et al., 1996), was recently proposed as a potential candidate for injectable anticoagulants, due to its potency, specificity of action, long-lasting activity, and safety profile. Hirunorms represent a novel class of multisite-directed thrombin inhibitors. They were rationally designed to interact with the thrombin active site in a nonsubstrate mode (hirudin-like binding mode), through their N-terminal end; they were also expected to specifically bind the fibrinogen recognition exosite, through their C-terminal domain. An appropriate spacer segment, able to posi-

Table 1. *Primary structure of hirunorm V and comparison with hirudin*[a]

Hirudin	Hirunorm V
$Ile^{1'}$	$Chg^{1''}$
$Thr^{2'}$	$Val^{2''}$
$Tyr^{3'}$	$2\text{-}Nal^{3''}$
$Thr^{4'}$	$Thr^{4''}$
$Asp^{5'}$	$Asp^{5''}$
|	D-$Ala^{6''}$
Globular domain	$Gly^{7''}$
|	β-$Ala^{8''}$
$Pro^{48'}$	$Pro^{9''}$
$Glu^{49'}$	$Glu^{10''}$
$Ser^{50'}$	$Ser^{11''}$
$His^{51'}$	$His^{12''}$
$Asn^{52'}$	h-$Phe^{13''}$
$Asx^{53'}$	$Gly^{14''}$
$Gly^{54'}$	$Gly^{15''}$
$Asp^{55'}$	$Asp^{16''}$
$Phe^{56'}$	$Tyr^{17''}$
$Glu^{57'}$	$Glu^{18''}$
$Glu^{58'}$	$Glu^{19''}$
$Ile^{59'}$	$Ile^{20''}$
$Pro^{60'}$	$Pro^{21''}$
$Glu^{61'}$	$Aib^{22''}$
$Glu^{62'}$	$Aib^{23''}$
$Tyr^{63'}$	$Tyr^{24''}$
$Leu^{64'}$	$Cha^{25''}$
$Gln^{65'}$	D-$Glu^{26''}$

[a]Recombinant hirudin variant 2, Lys^{47}, used as template structure for the design of hirunorm V (Rydel et al., 1991).

tion properly the N-terminal end of the inhibitor in the active site, was also designed. Hirunorms were proposed as true hirudin mimetics, not only because they share features with the hirudin sequence, but particularly because they were designed to bind thrombin in a hirudin-like mode, yet differently from fibrinogen, hirulogs, hirutonins, and other synthetic thrombin inhibitors. The proposed binding mode of hirunorms to thrombin, as compared to those of hirulogs and hirutonins, is reported schematically in Figure 1G.

Hirunorms were found to be strong inhibitors of the amidolytic activity of α-thrombin toward small chromogenic substrates: the most active molecules, hirunorms IV and V, showed the highest affinity for thrombin, with K_i values in the pM range. Moreover, the peculiar molecular structure of hirunorms makes them stable to the proteolytic action of thrombin, without the need for peptide bond modifications. Hirunorms display a high degree of selectivity, being unable to inhibit trypsin, plasmin, and tPa. As expected, hirunorms showed high potency in anticoagulant assays. Experimental pharmacology studies on hirunorm V show its effectiveness as anticoagulant agent, with antithrombotic properties, in different rat models. Hirunorm V is resistant to proteolysis and shows low plasma clearance; its elimination is less dependent on renal function than that of hirudin. Surprisingly, hirunorm V compares favorably with recombinant hirudin against arterial thrombosis and does not affect bleeding at antithrombotic doses (Lombardi et al., 1996).

In the present paper, we describe the crystal structure of hirunorm V in its complex with human α-thrombin, determined at 2.1 Å resolution (R-factor = 0.176), and we prove that its distinctive binding mode to the proteinases is that of a true low molecular weight hirudin mimetic.

Results and discussion

Thrombin structure

The three-dimensional structure of the thrombin molecule, observed in the complex with hirunorm V, is quite similar to those observed in other thrombin–inhibitor complexes reported in the literature (Bode et al., 1989; Iwanowicz et al., 1994; Tsuda et al., 1994; Tabernero et al., 1995; Féthière et al., 1996). When superimposing all the thrombin Cα atoms with those of the enzyme in the thrombin–hirudin complex (PDB code 4htc, Rydel et al., 1991; this structure is used throughout the text as reference thrombin–hirudin complex), an RMS deviation of 0.38 Å is observed. The largest deviations are localized in the Tyr^{60A}–Trp^{60D} insertion loop, which has been proposed as a chemotactic domain (Bar-Shavit et al., 1984). The side chains of residues Tyr^{60A} and of Trp^{60D} in the thrombin–hirunorm V complex are displaced by about 1.5 Å and 2.5 Å, respectively, from that of the thrombin–hirudin complex (the residue numbering in thrombin is based on the chymotrypsin sequence; Bode et al., 1989). Perturbation of the Tyr^{60A}–Trp^{60D} loop structure, formerly thought to be compact and rather rigid (Stubbs & Bode, 1993), has also been observed in the thrombin–Dmc-azaLys complex (Nardini et al., 1996).

The active site triad displays a geometry virtually indistinguishable, within the experimental errors, from that of the other members of the trypsin-like serine proteinase family. This indicates that the binding of the inhibitors in the active site does not affect the thrombin structure significantly. Weak or missing electron density, as for other thrombin complexes crystallized in the same monoclinic form, is observed for the A-chain (residues 1H-1C, 14L-15), B-chain (residues 246–247), and for the γ autolysis loop (residues 147–149E). Furthermore, Glu^{192}, close to the substrate recognition region, displays a poor side-chain electron density.

Hirunorm V structure

In agreement with the design hypothesis (Lombardi et al., 1996), hirunorm V (whose primary structure is reported in Table 1) is in contact with thrombin at two different sites. The electron density for the hirunorm V N-terminal tetrapeptide, bound to thrombin active site, is shown in Figure 2A, and the electron density for the C-terminal undecapeptide, bound to thrombin FRE, is reported in Figure 2B. Interpretable electron density for the segment (D-$Ala^{6''}$–$Gly^{15''}$), connecting the N-terminal tetrapeptide to the FRE-binding region, is absent from the Fourier maps calculated throughout this crystallographic analysis.

The N-terminal tetrapeptide of hirunorm V adopts an extended conformation; $Chg^{1''}$ and $2\text{-}Nal^{3''}$ side chains are contacting each other on the same side of the inhibitor polypeptide backbone, whereas $Val^{2''}$ and $Thr^{4''}$ side chains fall on the other side. The cyclohexyl ring of $Chg^{1''}$ adopts a typical chair conformation, with the Cα atom in the equatorial position. The $Val^{2''}$ residue adopts a typical *trans* (*gauche*(−)) χ^1 angle. The $2\text{-}Nal^{3''}$ shows a χ^1 *gauche*(−) and χ^2 *skew* conformation, as usually observed for the side-chain orientation of aromatic amino acids. $Thr^{4''}$ is locked in a *gauche*(+) (*gauche*(−)) side-chain conformation by an intrares-

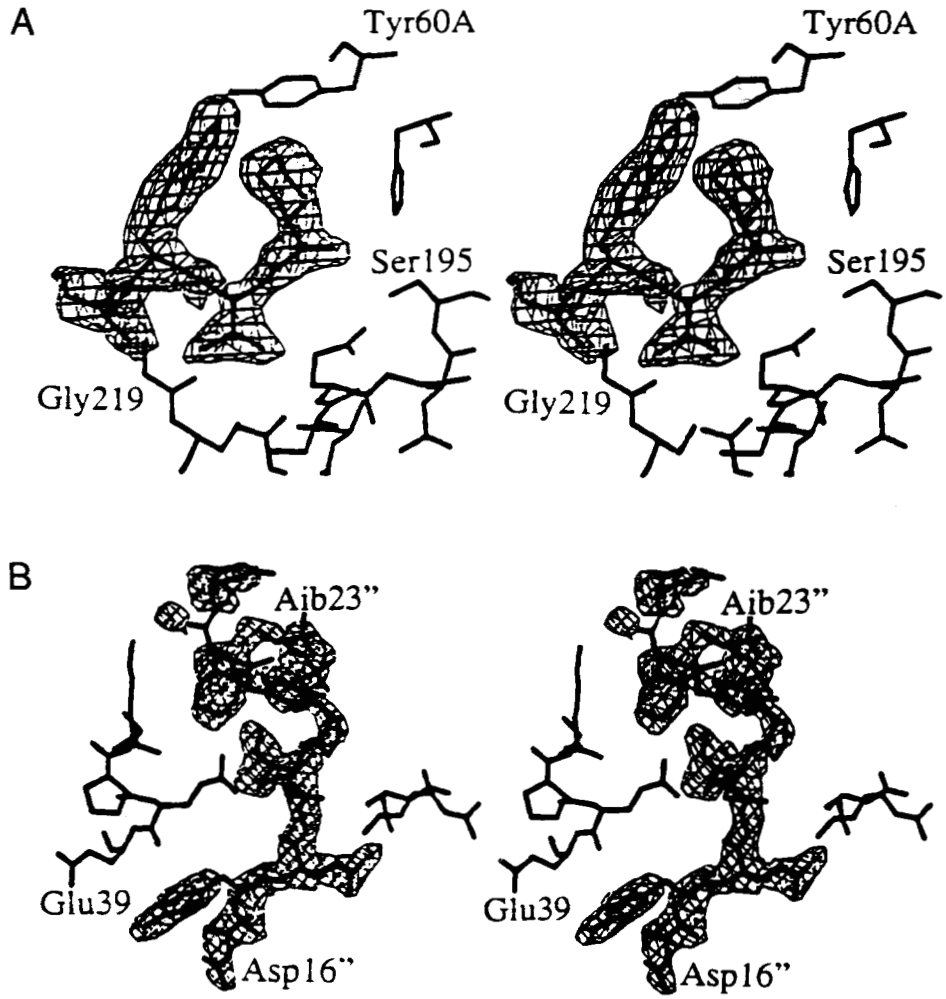

Fig. 2. Stereo views of the electron density map, contoured at 1σ, for the hirunorm V N-terminal tetrapeptide Chg$^{1''}$–Thr$^{4''}$ when bound to thrombin active site (**A**) and for the C-terminal hirunorm V undecapeptide Asp$^{16''}$–D-Glu$^{26''}$ when bound to thrombin FRE (**B**).

idue hydrogen bond between the OG and the carbonyl oxygen atoms (OG···O distance is 3.0 Å).

Because of the β-strand conformation and of the different bulkiness of the side chains, the N-terminal part is larger around the 2-Nal$^{3''}$ residue and smaller around the Chg$^{1''}$ residue. This shape may in part justify the orientation of the inhibitor N-terminal segment with respect to the precleavage subsites. The smaller Chg$^{1''}$ residue deeply penetrates in the well-confined thrombin S2 subsite, and it reaches at close contact Ser^{195}, whereas the larger 2-Nal$^{3''}$ residue is shortly outside the active site cavity. Hirunorm V N-terminal peptide backbone is parallel to the Ser^{214}–Gly^{219} thrombin segment. This alignment is rather unusual for serine proteinase–inhibitor interaction, and it was observed in thrombin–hirudin (Grütter et al., 1990; Rydel et al., 1990, 1991), in thrombin–BMS-183507 (Iwanowicz et al., 1994; Tabernero et al., 1995), and in thrombin–ornithodorin (van de Locht et al., 1996) complexes.

Four backbone to backbone hydrogen bonds stabilize the hirunorm V N-terminal tripeptide in the active site (Chg$^{1''}$N···Ser^{214}O, 3.1 Å; Chg$^{1''}$O···Gly^{216}N, 3.0 Å; 2-Nal$^{3''}$N···Gly^{216}O, 2.7 Å, 2-Nal$^{3''}$O···Gly^{219}N, 2.8 Å); Figure 3 shows the hirunorm V structure around the active site, in comparison with the thrombin–hirudin complex.

Chg$^{1''}$ N atom shows potential interactions with the residues from thrombin catalytic triad. It is weakly hydrogen bonded to Ser^{195}OG (3.5 Å), and is 3.2 Å apart from His^{57}NE2. The Chg$^{1''}$ residue is in van der Waals contact with the imidazole ring of His^{57} (Chg$^{1''}$N···His^{57}CD2, 3.9 Å; Chg$^{1''}$N···His^{57}CE1, 3.7 Å; Chg$^{1''}$CG1···His^{57}CD2, 3.8 Å) and with Ser^{195}CB (4.0 Å). The cyclohexyl ring faces *edge on* the Tyr^{60A} phenyl ring and *side on* the Trp^{60D} indolyl ring. It is also in van der Waals contact with Leu^{99} side chain (Chg$^{1''}$CG2···Leu^{99}CD1, 3.9 Å), which adopts a common staggered conformation ($\chi^{2,1}$ and $\chi^{2,2}$ values are $-164°$ and $-34°$, respectively). This side-chain conformation is different from the rarely occurring *skew* conformation observed for Leu^{99} in the thrombin–hirudin complex (whose Leu^{99} $\chi^{2,1}$ and $\chi^{2,2}$ values are 12° and 131°, respectively). Thus, the cyclohexyl ring fills almost completely the hydrophobic cavity (S2 subsite) defined by Leu^{99}, His^{57}, Tyr^{60A}, and Trp^{60D}, as shown in Figure 4A, where the S2 subsite from the thrombin–hirudin complex (hosting Ile$^{1'}$) is also displayed (Fig. 4B). The small structural perturbations observed in the 60-insertion loop, with respect to the thrombin–hirudin complex, may be caused by the optimization of the contacts with the Chg$^{1''}$ residue. Val$^{2''}$ side chain is at van der Waals contact with residues Gly^{219}, Cys^{220}, and Glu^{192} of thrombin. These res-

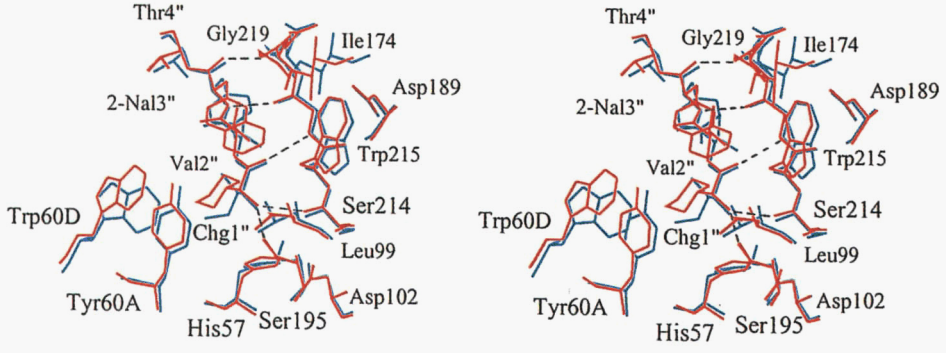

Fig. 3. Detailed description in stereo view of the active site binding region of hirunorm V (red) superimposed with thrombin–hirudin complex (blue). Dashed lines indicate hydrogen bonds.

idues define a rim at the entrance of the S1 specificity subsite. The subsite, however, does not host an inhibitor residue, although the side chain of $Val^{2''}$ points toward it, as observed in the thrombin–hirudin complex. The $2\text{-}Nal^{3''}$ residue occupies the secondary aryl binding site. An *edge-on* interaction between $2\text{-}Nal^{3''}$ naphtyl ring and Trp^{215} indolyl ring is observed (the closest contact is $2\text{-}Nal^{3''}CF2 \cdots Trp^{215}CD2$, 3.7 Å). The naphtyl ring is also at van der Waals contact with Ile^{174} and Tyr^{60A}. Figure 5 depicts the orientation of $2\text{-}Nal^{3''}$ (Fig. 5A) in comparison with $Tyr^{3'}$, in the thrombin–hirudin complex (Fig. 5B). In summary, in the hirunorm V N-terminal region, the $Chg^{1''}$ residue is located in the S2 hydrophobic subsite, $Val^{2''}$ approximates the S3 subsite (Stubbs & Bode, 1995) and $2\text{-}Nal^{3''}$ occupies the aryl binding site.

A comparison of hirunorm V with hirudin–thrombin (Rydel et al., 1991), and BMS-183507–thrombin (Tabernero et al., 1995) complexes, which share the common nonsubstrate-like binding mode, is shown in Figure 6A. The structural agreement between the backbones of hirunorm V and of the hirudin N-terminal tripeptide is remarkable. Such a coincidence indicates, in agreement with the design hypothesis, that the hydrophobic S2 subsite and the aryl binding site of thrombin are more completely filled by a cyclohexyl ring and a naphtyl ring, respectively, as in hirunorm V, rather than by an isobutyl and a phenoxy group, which are present in the hirudin N-terminal segment (see also Figs. 4, 5).

BMS-183507 (Tabernero et al., 1995) is also a retrobinding inhibitor, but the location of its peptide backbone deviates signif-

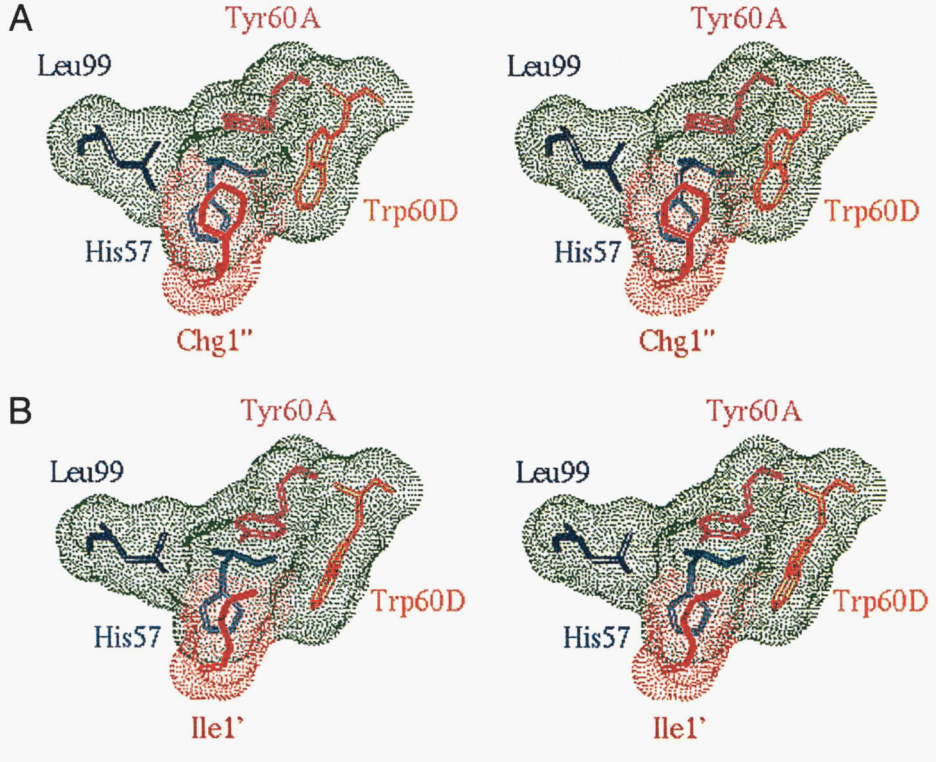

Fig. 4. S2 site region of the complex thrombin–hirunorm V (**A**) and thrombin–hirudin (**B**) with the Connolly surface representation.

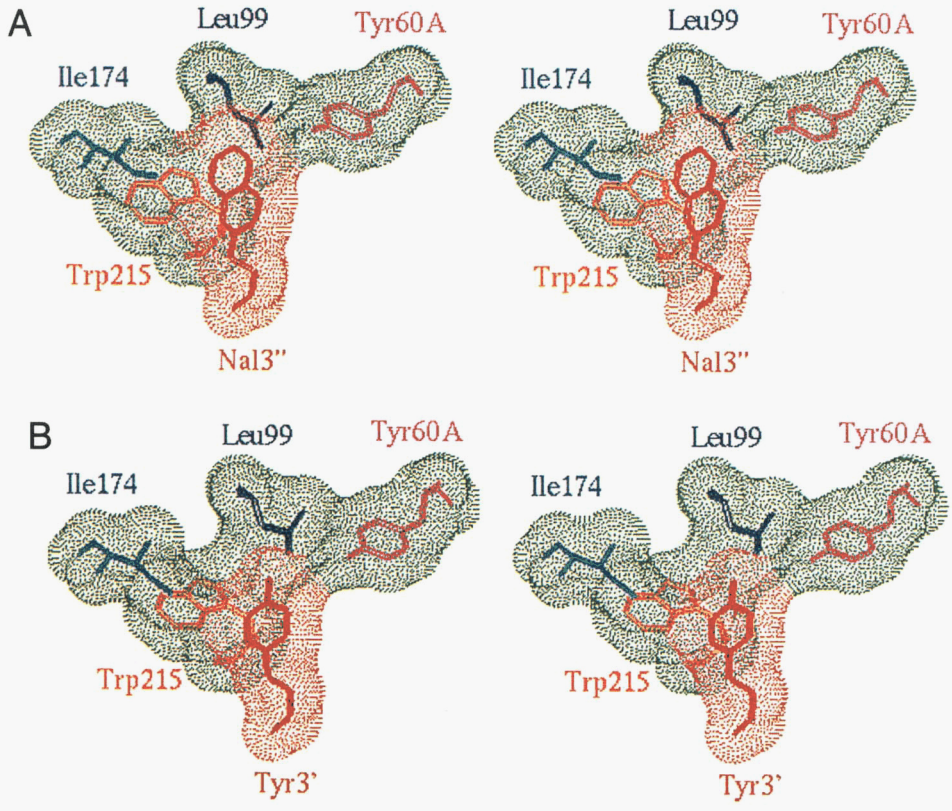

Fig. 5. Aryl binding site region of the complex thrombin–hirunorm V (**A**) and thrombin–hirudin (**B**) with the Connolly surface representation.

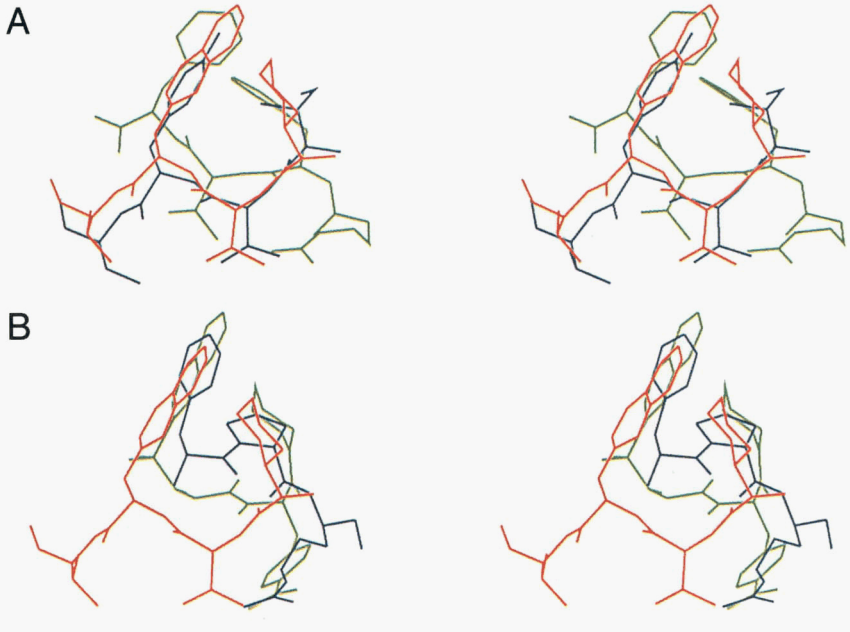

Fig. 6. A: Stereo view of the backbone atoms superimposition of hirunorm V $Chg^{1''}$–$Thr^{4''}$ N-terminal segment (red) with hirudin segment $Ile^{1'}$–$Thr^{4'}$ (blue) and BMS-183507 (green). **B:** Stereo view of the backbone atoms superimposition of hirunorm V from $Chg^{1''}$ to $Thr^{4''}$ (red) with hirulog 1 from D-$Phe^{1'}$ to $Arg^{3'}$ (blue) and NAPAP (green).

icantly from those of hirudin and hirunorm V (see Fig. 6A). BMS-183507 contains a guanidinium group at the N-terminal end, which is ready to interact with Asp^{189}. This ionic interaction forces a slight rotation of the entire inhibitor molecule to displace BMS-183507 residue Thr^{3} with respect to $Val^{2''}$ and $Thr^{2'}$ (in hirunorm V and hirudin, respectively), while keeping in approximately unperturbed positions Phe^{2} (in S2) and Phe^{4} (in the adjacent aryl binding site) (see Fig. 6A).

Figure 6B shows an overlay of the thrombin-bound hirulog 1 (Skrzypczak-Jankun et al., 1991), NAPAP (Brandstetter et al., 1992) and hirunorm V inhibitors. Analysis of the figure shows that the distinctive nonsubstrate-like binding mode of hirunorm V differs substantially from the substrate-like binding mode adopted by hirulog 1 and by NAPAP. Nevertheless, despite the opposite inhibitor backbone orientations and the different locations, the S2 subsite and the aryl binding site are similarly occupied by the three inhibitors.

Quite surprisingly, the designed hirunorm V $Asp^{5''}$–$His^{12''}$ linker segment is not defined by continuous electron density, presumably due to high flexibility. Poorly defined electron density is also observed for the region corresponding to the h-$Phe^{13''}$–$Gly^{15''}$ segment, which was model-built in extended conformation.

Flexibility of this part of the molecule was also observed in thrombin–hirudin (Grütter et al., 1990; Rydel et al., 1990, 1991; Vitali et al., 1992) and thrombin–hirulog (Skrzypczak-Jankun et al., 1991; Qiu et al., 1992) complexes, and was attributed to a nonenzymatic deamination of $Asn^{53'}$ (Qiu et al., 1992). Because hirunorm V does not contain any Asn residue, the observed flexibility can be attributed tentatively to the lack of thrombin–inhibitor interactions in this zone and/or to an inappropriate size of the linker segment. In fact, a shorter linker, displaying several interactions with thrombin surface, is well organized in hirutonin 6 (Zdanov et al., 1993).

However, it is worth mentioning that the distance between $Thr^{4''}C\alpha$ atom and $Asp^{16''}C\alpha$ atom is 25.6 Å, as expected from the initial model.

In the C-terminal half of the hirunorm V molecule, the electron density is well defined in the $Asp^{16''}$–$Pro^{21''}$ region (except for the side chain of $Glu^{19''}$). These residues bind tightly to the FRE in extended conformation. As observed for many other complexes bearing a FRE recognition moiety, residues $Tyr^{17''}$ and $Ile^{20''}$ are particularly well ordered (Rydel et al., 1991; Skrzypczak-Jankun et al., 1991; Berliner, 1992; Zdanov et al., 1993). Indeed, the binding mode of this fragment to the FRE is similar to that of other bifunctional inhibitors containing the same motif, with a characteristic pattern of hydrophobic interactions involving $Tyr^{17''}$ and $Ile^{20''}$. Direct ion pairing between $Asp^{16''}$ and Arg^{73} ($Asp^{16''}OD1 \cdots Arg^{73}$ NH1, 2.9 Å; $Asp^{16''}OD2 \cdots Arg^{73}$ NH2, 3.8 Å), and electrostatic interactions involving $Glu^{18''}$, $Glu^{19''}$, D-$Glu^{26''}$ and Arg^{67}, Arg^{73}, Arg^{75}, Arg^{77A}, Lys^{36}, Lys^{81}, Lys^{109}, Lys^{110} may also contribute to the tight binding and to the structuring of this extended region of the inhibitor. Moreover, the electron density around the expected location of the C-terminal part ($Aib^{22''}$–D-$Glu^{26''}$) is weak, although compatible with a 3_{10}-helical conformation. In this particular conformation, the side chain of $Cha^{25''}$ would be placed at van der Waals contact with $Ile^{20''}$, at the site of hirudin $Leu^{64'}$, which is also part of a 3_{10}-helical turn in the thrombin–hirudin complex. No density is observed for D-$Glu^{26''}$. In Figure 7 is shown the stereo view of the superimposition of hirudin$^{55'\text{-}65'}$ and hirunorm $V^{16''\text{-}26''}$ as they are bound in the fibrinogen exosite of thrombin.

A space-filling representation of thrombin–hirunorm V complex, highlighting the tight enzyme–inhibitor contact, is shown in Figure 8.

Solvent structure and inhibitor binding

Analysis of the solvent molecules localized in the thrombin–hirunorm V complex shows, as expected, an overall agreement with the solvent structure for the related thrombin–hirudin com-

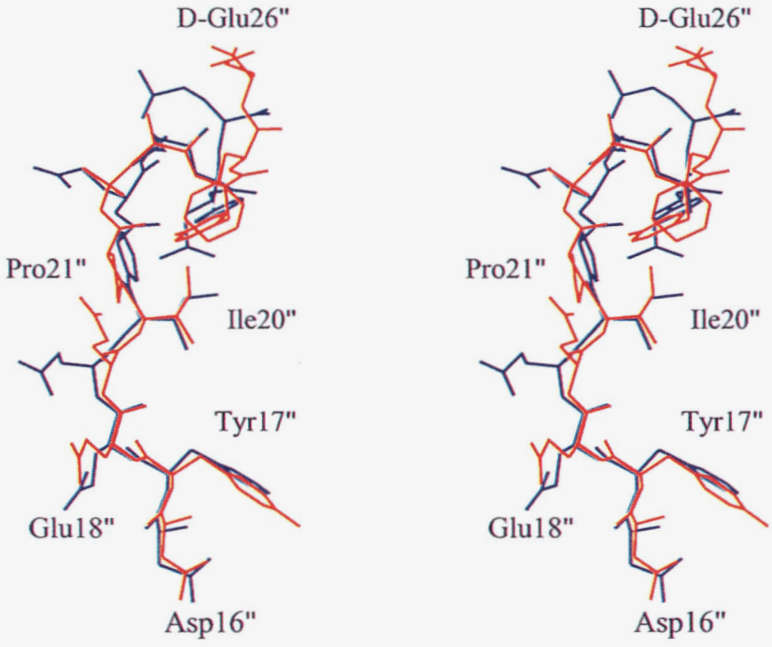

Fig. 7. Stereo view of the superimposition of hirudin$^{55'\text{-}65'}$ and hirunorm $V^{16''\text{-}26''}$ as they are bound in the fibrinogen exosite of thrombin.

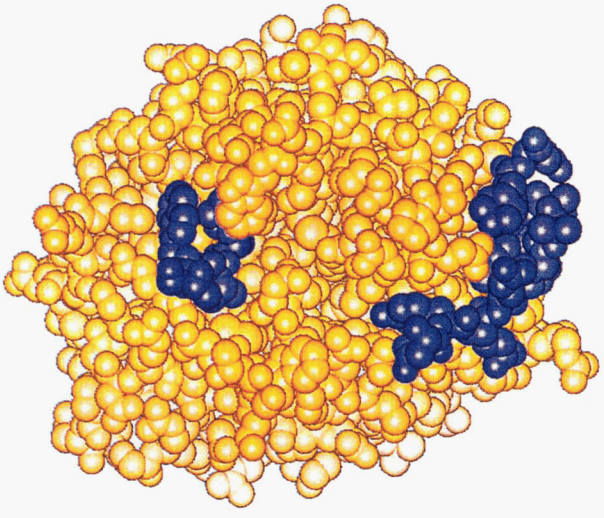

Fig. 8. Space-filling representation of thrombin–hirunorm V complex.

plex reported previously (Rydel et al., 1991). It is, however, worth pointing out that the apolar nature of the N-terminal region of hirunorm V may have a favorable effect on its association process to thrombin, through a consistent release of surface-bound water molecules, from the complex, to the bulk solvent. In particular, from a comparison of the crystal structures of thrombin–hirunorm V and thrombin–hirudin (see Fig. 9), it appears that water molecules W432, which is hydrogen bonded to $Tyr^{3'}$ (3.2 Å), and W606, which bridges $Tyr^{60A}OH$ (2.4 Å) and $Tyr^{3'}OH$ (3.0 Å) when hirudin is bound (Rydel et al., 1991), are displaced by the bulky naphtyl ring of hirunorm V 2-$Nal^{3''}$ residue. Moreover, the presence of residue $Val^{2''}$, substituting for $Thr^{2'}$ of hirudin, does not allow to stabilize the surface water molecule W410 (W410···$Thr^{2'}$OG, 2.8 Å). In thrombin–hirudin complex, this W410 water molecule further stabilizes on the thrombin surface through hydrogen bonding two additional water molecules: W579 and W538. The W410···W579 distance is particularly short (2.0 Å) and the distance W579···W538 is 2.6 Å (Rydel et al., 1991). As expected for multisite-directed thrombin inhibitors, similar surface water displacement processes, contributing to complex stability through an increase in the solvent entropy, take place in the FRE region, which is filled by an extended and tightly binding inhibitor segment (Bode et al., 1992a; Ascenzi et al., 1995; van de Locht et al., 1995, 1996; Engh et al., 1996; Salemme et al., 1997).

Conclusions

The present structural analysis, together with the previous design and functional inhibition studies (Lombardi et al., 1996), shows, for the first time to our knowledge, that true hirudin mimetic inhibitors can be designed, achieving picomolar affinities for thrombin. This observation bears practical implications for the design of selective anticoagulant and antithrombotic drugs. Key structural elements in such design are the choice of the FRE and active site-directed molecular fragments, as well as of a suitable linker segment, connecting the two parts.

It should be noted that no structural analogues of hirunorms are known within natural polypeptidic thrombin inhibitors. Indeed, in free hirudin (and in antistasin, ghilanten, decorsin, ornatin, and hirustasin; see Ascenzi et al., 1995), the N-terminal retro-binding tripeptide makes part of a well-structured, small, globular domain, stabilized by three disulfide bridges, which is followed by the extended FRE-binding C-terminal region (Bode et al., 1992a). Moreover, in the two-headed inhibitor ornithodorin, a more complex binding scheme is adopted, in that thrombin active site retro-binding and FRE binding peptide segments are provided by two distinct and properly structured globular domains, which adopt a Kunitz-inhibitor fold, and are organized in a tandem repeat (van de Locht et al., 1996).

A key functional property required for serine proteinase inhibitors to be used in therapy is a low cross-reactivity with enzymes from the same homology family, which are active in different, but

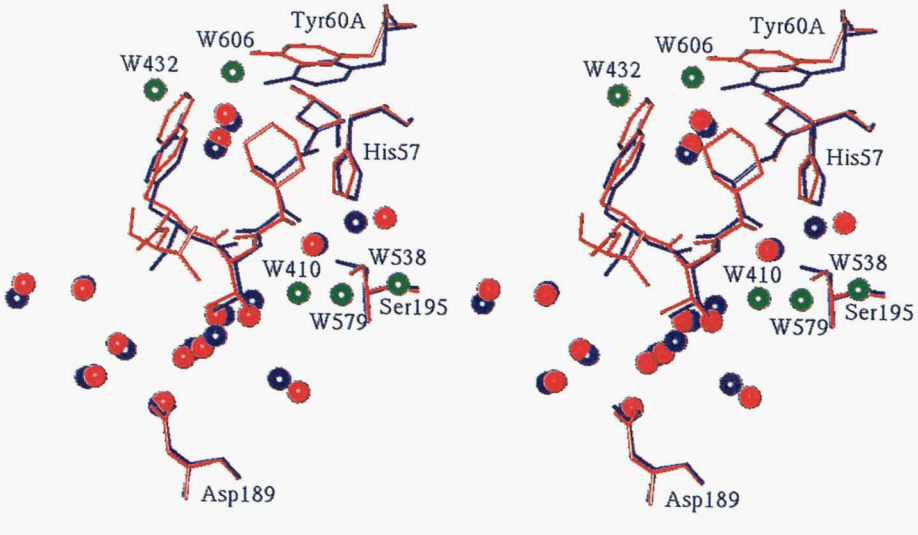

Fig. 9. Stereo view of the water structure near the S1 site, the catalytic triad of thrombin, the hydrophobic pocket S2, and the aryl binding site. Red, atoms belonging to thrombin–hirunorm V complex; blue, atoms belonging to thrombin–hirudin complex; green, water molecules that are present in thrombin–hirudin complex but absent in thrombin–hirunorm V complex.

crucial, metabolic compartments. The strong inhibitory selectivity displayed by hirunorms stems from the pairing of two unique molecular features, the active site retro-binding and the FRE-binding segments, which, as in hirudin and hirudin-related inhibitors, help to select their target proteinase. As a comparison, it could be considered that active site-directed thrombin inhibitors (i.e., lacking a FRE binding tail), such as BMS-183507 (a retro-binding peptide analogue; Tabernero et al., 1995), BMS-186282, or BMS-189090 (substrate-like binding, Malley et al., 1996), bind to thrombin with nanomolar affinities, and display much lower selectivities toward trypsin, plasmin, and tPa. Finally, related to the active site binding mode, it should also be considered that retro-binding, with unproductive location of the inhibitor backbone with respect to the S1 subsite and to the proteinase catalytic triad, is the structural basis for the stability of hirunorms to proteolysis (Lombardi et al., 1996).

Materials and methods

Preparation of the crystals

A protein solution was prepared initially using human α-thrombin (about 1 mg/mL) (Calbiochem) in 0.02 M Tris-HCl, at pH 7.4 and 0.1 M sodium chloride. The complex with hirunorm V was formed by adding a 10-molar excess of the peptide (synthesized as reported previously by Lombardi et al., 1996) to the thrombin solution. The mixture was incubated for 2 h at room temperature, concentrated, and the buffer exchanged with a solution of 0.05 M sodium phosphate at pH 6.0 and 0.75 M in sodium chloride. The final concentration of the complex was 20 mg/mL.

Crystals of the thrombin–hirunorm V complex were grown using a cross-seeding technique (Stura & Wilson, 1992). First, crystals of thrombin–hirugen complex were grown, as described by Skrzypczak-Jankun et al. (1991), by vapor diffusion methods at 4 °C: 6-μL drops, containing 0.05 M sodium Hepes, pH 7.0, 10% (w/v) PEG 4000, 0.02% NaN_3, 12 mg/mL thrombin–hirugen complex were equilibrated against a precipitating solution containing 0.1 M sodium Hepes, pH 7.0, 20% (w/v) PEG 4000, 0.04% NaN_3. Large single crystals of this complex were obtained, harvested, and washed twice with reservoir solution. One crystal was then crushed into individual seeds (about 10 μm). These seeds were transferred into drops of a solution containing the thrombin–hirunorm V complex. This solution had been equilibrated for four days prior to seeding.

The composition of the solutions used for the growing of the thrombin–hirunorm V crystals was identical to that used for thrombin–hirugen complex. The seeds grew to 0.1 mm * 0.1 mm * 0.1 mm dimensions within two weeks. The crystals obtained from cross-seeding were washed and crushed and used in another cross-seeding experiment. These new crystals were used for macroseeding experiments.

Data collection and processing

Data collection was performed with a Rigaku R-axis-II imaging plate system (Molecular Structure Corp., Houston, Texas, USA) using CuKα radiation, and one crystal of dimensions 0.3 mm * 0.4 mm * 0.4 mm. A total of 54,776 reflections were measured, and reduced to 21,615 unique reflections, which correspond to a completeness of 99.4% in the 20.0–2.1 Å resolution range (R_{sym} = 0.072). Diffracted intensities were processed using MOSFLM (Leslie, 1992) and programs from the CCP4 program suite (CCP4, 1994). The crystal employed belongs to the monoclinic space group C2 with unit cell constants: a = 71.9 Å, b = 72.8 Å, c = 73.3 Å, and β = 100.7°, one complex moiety per asymmetric unit.

Crystallographic refinement

The structure of the thrombin–hirunorm V complex was analyzed by difference Fourier techniques. Atomic coordinates of the thrombin–hirugen complex were recovered from the Brookhaven Protein Data Bank (Bernstein et al., 1977; Abola et al., 1987) as data set 1hah (Vijayalakshmi et al., 1994). Water and hirugen molecules were removed from the starting model prior to structure factor and phase calculation. The crystallographic R-factor, calculated in the 20.0–2.1-Å resolution range, based on the starting model coordinates, was 0.340. Fourier maps, calculated with $2F_o - F_c$ and $F_o - F_c$ coefficients (F_o are the observed structure factors for the complex, and F_c are those calculated on the basis of the model atomic coordinates) showed prominent electron density features in the active site and in the exosite regions of thrombin. After an initial refinement, limited to the enzyme structure (R-factor 0.218), a preliminary model for the N-terminal and C-terminal segments of hirunorm V was easily built and introduced in the atomic coordinates set for further refinement, which proceeded to convergence with continuous map inspection and model updates. Solvent molecules were included if identified by peaks of difference electron density with value above 3.0 σ, and if engaged in hydrogen bonds. The electron density maps were calculated using programs from the CCP4 suite (CCP4, 1994) and the structure refinement was performed using TNT (Tronrud et al., 1987). Map inspection and model correction during refinement were based on the graphics program O (Jones et al., 1991).

The final crystallographic R-factor calculated for all the 21,615 observed reflection (in the 20.0–2.1-Å resolution range) is 0.176. The refined model includes 2,323 protein atoms, 104 atoms belonging to the inhibitor, and 134 water molecules. The RMS deviations of bond lengths and bond angles from ideal values (Engh & Huber, 1991) are 0.018 Å and 2.8°, respectively. Atomic coordinates and observed structure factors for thrombin–hirunorm V complex have been deposited with the Brookhaven Protein Data Bank (Bernstein et al., 1977; Abola et al., 1987) (entry code 5gds).

Acknowledgments

We thank Prof. A. Coda, Drs. M. Rizzi and C. Tarricone for several helpful suggestion during different stages of the analysis. This study was partially supported by grants from the Ministry of University, Scientific Research and Technology of Italy (MURST), from the National Research Council of Italy (CNR), and from the European Union Capital Mobility Program "Advanced Methods for the Crystallography of Biological Macromolecules" (grant CT940690).

References

Abola EE, Bernstein FC, Bryant SH, Koetzle TF, Weng J. 1987. Protein Data Bank. In: Allen FH, Bergerhoff G, Sievers R, eds. *Crystallographic databases—Information content, software systems, scientific applications.* Bonn/Cambridge/Chester: Data Commission of the International Union of Crystallography. pp 107–132.

Ascenzi P, Amiconi G, Bode W, Bolognesi M, Coletta M, Menegatti E. 1995. Proteinase inhibitors from the European medicinal leech *Hirudo medicinalis*: Structural functional and biomedical aspects. *Mol Aspects Med 16*:215–313.

Banner DW, Hadvary P. 1991. Crystallographic analysis at 30 Å resolution of the binding to human thrombin of four active site-directed inhibitors. *J Biol Chem 266*:20085–20093.

Bar-Shavit R, Kahn A, Wilner GD, Mann KG, Fenton JW II. 1984. Localization of a chemotactic domain in human thrombin. *Biochemistry 23*:397–400.

Berliner LJ. 1992. *Thrombin structure and function.* New York: Plenum Press.

Bernstein FC, Koetzle TF, Williams GJB, Meyer EF Jr, Brice MD, Rodgers JR, Kennard O, Shimanouchi T, Tasumi M. 1977. The Protein Data Bank: A computer-based archival file for macromolecular structures. *J Mol Biol 112*:535–542.

Bode W, Huber R. 1992. Natural protein proteinase inhibitors and their interaction with proteinases. *Eur J Biochem 204*:443–452.

Bode W, Huber R, Rydel TJ, Tulinsky A. 1992a. X-ray crystal structures of human α-thrombin and of human thrombin-hirudin complex. In: Berliner LJ, ed. *Thrombin structure and function.* New York: Plenum Press.

Bode W, Mayr I, Baumann U, Huber R, Stone SR, Hofsteenge J. 1989. The refined 1.9 Å crystal structure of human α-thrombin: Interaction with D-Phe-Pro-Arg-chloromethylketone and significance of the Tyr-Pro-Pro-Trp insertion segment. *EMBO J 8*:3467–3475.

Bode W, Turk D, Karshikov A. 1992b. The refined 1.9 Å X-ray crystal structure of D-Phe-Pro-Arg chloromethylketone-inhibited human α-thrombin: Structure analysis, overall structure, electrostatic properties, detailed active-site geometry, and structure–function relationships. *Protein Sci 1*:426–471.

Brandstetter H, Turk D, Hoeffken HW, Grosse D, Stürzebecher J, Martin PD, Edwards BFP, Bode W. 1992. Refined 2.3 Å X-ray crystal structure of bovine trombin complexes formed with the benzamidine and arginine-based thrombin inhibitors NAPAP 4-TAPAP and MQPA. *J Mol Biol 226*:1085–1099.

CCP4. 1994. The CCP4 suite: Programs for protein crystallography *Acta Crystallogr D 50*:760–767.

Davie EW, Fujikawa K, Kisiel W. 1991. The coagulation cascade: Initiation maintenance and regulation. *Biochemistry 30*:10364–10370.

DiMaio J, Gibb B, Munn D, Lefebre J, Ni F, Konishi Y. 1991. A new class of potent thrombin inhibitors that incorporates a scissile pseudopeptide bond. *FEBS Lett 282*:47–52.

DiMaio J, Gibb B, Lefebre J, Konishi Y, Munn D, Yue SY. 1992. Synthesis of a homogeneous series of ketomethylene arginyl pseudopeptides and application to low molecular weight hirudin-like thrombin inhibitors. *J Med Chem 35*:3331–3341.

Engh RA, Huber R. 1991. Accurate bond and angle parameters for X-ray protein structure refinement. *Acta Crystallogr A 47*:392–400.

Engh RA, Brandstetter H, Sucher G, Eichinger A, Baumann U, Bode W, Huber R, Poll T, Rudolph R, von der Saal W. 1996. Enzyme flexibility solvent and "weak" interactions characterize thrombin-ligand interactions: Implication for drug design. *Structure 4*:1353–1362.

Fenton JW II. 1986. Thrombin. *Ann NY Acad Sci 485*:5–15.

Fenton JW II, Bing DH. 1986. Thrombin active-site regions. *Semin Thromb Haemostasis 12*:200–208.

Fenton JW II, Ofosu FA, Moon DG, Maraganore JM. 1991. Thrombin structure and function: Why thrombin is the primary target for antithrombotics. *Blood Coag Fibrinol 2*:69–75.

Fenton JW II, Olson TA, Zabinski MP, Wilner GD. 1988. Anion binding exosite of human α-thrombin and fibrinogen recognition. *Biochemistry 27*:7106–7112.

Féthière J, Tsuda Y, Coulombe R, Konishi Y, Cygler M. 1996. Crystal structure of two new bifunctional nonsubstrate type thrombin inhibitors complexed with human α-thrombin. *Protein Sci 5*:1174–1183.

Grütter MG, Priestle JP, Rahuel J, Grossenbacher H, Bode W, Hofsteenge J, Stone SR. 1990. Crystal structure of the thrombin–hirudin complex: A novel mode of serine proteinase inhibition. *EMBO J 9*:2361–2365.

Iwanowicz E, J Lau WF, Lin J, Roberts DGM, Seiler SM. 1994. Retro-binding tripeptide thrombin active-site inhibitors: Discovery synthesis and molecular modeling. *J Med Chem 37*:2122–2124.

Jakubowski JA, Maraganore JM. 1990. Inhibition of coagulation and thrombin induced platelet activities by a synthetic dodecapeptide modeled on the carboxy terminus of hirudin. *Blood 75*:399–406.

Jones TA, Zou JY, Cowan S, Kieldgaard M. 1991. Improved methods for building protein models in electron density maps and location of errors in these models. *Acta Crystallogr A 47*:110–119.

Kikumoto R, Tamao Y, Tezuka T, Tonomura S, Hara N, Ninomiya K, Hijikata A, Okamoto S. 1984. Selective inhibition of thrombin by 2R,4R-4-methyl-1-N2-[3-methyl-1,2,3,4-tetrahydro-8-quinolinyl sulphonyl-L-arginyl]-2-piperidine-carboxylic. *Biochemistry 23*:85–89.

Kline T, Hammond C, Bourdan P, Maraganore J. 1991. Hirulog peptides with scissile bond replacements resistant to thrombin cleavage. *Biochem Biophys Res Commun 177*:1049–1055.

Krishnan R, Tulinsky A, Vlasuk GP, Pearson D, Vallar P, Bergum P, Brunck TK, Ripka WC. 1996. Synthesis structure and structure–activity relationships of divalent thrombin inhibitors containing an α-keto-amide transition state mimetic. *Protein Sci 5*:422–433.

Krstenansky JL, Broersma RJ, Owen TJ, Payne MH, Yates MT, Mao SJ. 1990a. Development of MDL 28050 a small antithrombin agent based on a functional domain of the leech protein hirudin. *Thromb Haemostasis 63*:208–214.

Krstenansky JL, Mao SJT. 1987. Antithrombin properties of C-terminus of hirudin using synthetic unsulfated N^{α}-acetyl-hirudin 45–65. *FEBS Lett 211*:10–16.

Krstenansky JL, Owen TJ, Yates MT, Mao SJT. 1987. Anticoagulant peptides: Nature of the interaction of the C-terminal region of hirudin with a noncatalytic binding site of thrombin. *J Med Chem 30*:1688–1691.

Krstenansky JL, Owen TJ, Yates MT, Mao SJT. 1988. Design synthesis and antithrombin activity for conformationally restricted analogs of peptide anticoagulants based on the C–terminal region of the leech peptide hirudin. *Biochim Biophys Acta 957*:53–59.

Krstenansky JL, Owen TJ, Yates MT, Mao SJT. 1990b. The C-terminal binding domain of hirullin P18 antithrombic activity and comparison to hirudin peptides. *FEBS Lett 269*:425–429.

Laskowski M, Kato I. 1980. Protein inhibitors of proteinases. *Annu Rev Biochem 49*:593–626.

Leslie AGW. 1992. *Joint CCP4 and ESF-EACBM newsletter on protein crystallography no. 26.* Warrington, UK: Daresbury Laboratory.

Lombardi A, Nastri F, Della Morte R, Rossi A, De Rosa A, Staiano N, Pedone C, Pavone V. 1996. Rational design of true hirudin mimetics: Synthesis and characterization of multisite-directed α-thrombin inhibitors. *J Med Chem 39*:2008–2017.

Malley MF, Tabernero L, Chang CY, Ohringer SL, Roberts DGM, Das J, Sack JS. 1996. Crystallographic determination of the structures of human α-thrombin complexed with BMS-186282 and BMS-189090. *Protein Sci 5*:221–228.

Maraganore JM, Bourdon P, Jablonski J, Ramachandran KL, Fenton JWII. 1990. Design and characterization of hirulogs: A novel class of bivalent peptide inhibitors of thrombin. *Biochemistry 29*:7095–7101.

Markwardt F. 1994. The development of hirudin as an antithrombotic drug. *Thrombosis Res 74*:1–23.

Maryanoff BE, Qiu X, Padmanabhan KP, Tulinsky A, Almond HR Jr, Andrade-Gordon P, Greco MN, Kauffman JA, Nicolau KC, Liu A, Brungs PH, Fusetani N. 1993. Molecular basis for the inhibition of human α-thrombin by the macrocyclic peptide cyclotheonamide A. *Proc Natl Acad Sci USA 90*:8048–8052.

Mathews II, Padmanabhan KP, Ganesh V, Tulinsky A, Isshii M, Chen J, Turck CW, Coughlin SR. 1994. Crystallographic structures of thrombin complexed with thrombin receptor peptides: Existence of expected and novel binding modes. *Biochemistry 33*:3266–3279.

Nakanashi H, Chrusciel RA, Sheen R, Bertenshaw S, Johnson ME, Ryedel TJ, Tulinsky A, Kahn M. 1992. Peptide mimetics of the thrombin-bound structure of fibrinopeptide A. *Proc Natl Acad Sci USA 89*:1705–1709.

Nardini M, Pesce A, Rizzi M, Casale E, Ferraccioli R, Balliano G, Milla P, Ascenzi P, Bolognesi M. 1996. Human α-thrombin inhibition by the active site titrant N^{α}-NN-dimethylcarbamoyl-α-azalysine p-nitrophenyl ester: A comparative kinetic and X-ray crystallographic study. *J Mol Biol 258*:851–859.

Okamoto S, Hijikata A, Kikumoto R, Tonomura S, Hara N, Ninomiya K, Maruyama A, Sugano M, Tamao Y. 1981. Potent inhibition of thrombin by the newly synthesized arginine derivative no. 805. The importance of stereostructure of its carboxamide portion. *Biochem Biophys Res Commun 101*:440–446.

Priestle JP, Rahuel J, Rink H, Tones M, Grütter MG. 1993. Changes in interaction in complexes of hirudin derivatives and human α-thrombin due to different crystal forms. *Protein Sci 2*:1630–1642.

Qiu X, Padmanabhan KP, Carperos VE, Tulinsky A, Kline T, Maraganore JM, Fenton JW II. 1992. Structures of hirulog 3-thrombin complex and nature of S′ subsites of substrates and inhibitors. *Biochemistry 31*:11689–11697.

Qiu X, Yin M, Padmanabhan KP, Krstenansky JL, Tulinsky A. 1993. Structures of thrombin complexes with a designed and a natural exosite peptide inhibitor. *J Biol Chem 268*:20318–20326.

Rydel TJ, Ravichandran KG, Tulinsky A, Bode W, Huber R, Roitsch C, Fenton JW. 1990. The structure of a complex of recombinant hirudin and human α-thrombin. *Science 249*:277–280.

Rydel TJ, Tulinsky A, Bode W, Huber R. 1991. Refined structure of the hirudin–thrombin complex. *J Mol Biol 221*:583–601.

Salemme FR, Spurlino J, Bone R. 1997. Serendipity meets precision: The integration of structure-based drug design and combinatorial chemistry for efficient drug discovery. *Structure 5*:319–324.

Schechter I, Berger A. 1967. On the size of the active site in proteinases I papain. *Biochem Biophys Res Commun 27*:157–162.

Skrzypczak-Jankun E, Carperos VE, Ravichandran KG, Tulinsky A, Westbrook

M, Maraganore JM. 1991. Structure of hirugen and hirulog 1 complexes of α-thrombin. *J Mol Biol 221*:1379–1393.

Stone SR, Hofsteenge J. 1986. Kinetic of the inhibition of thrombin by hirudin. *Biochemistry 25*:4622–4628.

Stubbs MT, Bode W. 1993. A player of many parts: The spotlight falls on thrombin's structure. *Thromb Res 69*:1–58.

Stubbs MT, Bode W. 1995. Structure and specificity in coagulation and its inhibition. *Trends Cardiovasc Med 5*:157–166.

Stubbs MT, Oschkinat H, Mayr I, Huber R, Angliker H, Stone SR, Bode W. 1992. The interaction of thrombin with fibrinogen. A structural basis for its specificity. *Eur J Biochem 206*:187–195.

Stura EA, Wilson IA. 1992. Seeing techniques. In: Ducruix A, Giegé R, eds. *Crystallization of nucleic acids and proteins: A practical approach*. Oxford, UK: Oxford University Press. pp 99–126.

Stürzebecher J, Markwardt F, Voigt B, Wagner G. 1984. Inhibition of bovine and human thrombins by derivatives of benzamidines. *Thromb Res 36*:457–467.

Stürzebecher J, Markwardt F, Voigt B, Wagner G, Walsmann P. 1983. Cyclic amides of Na-arylsulfonylamino acylated 4-amidinophenylalanine—Tight binding of thrombin. *Thromb Res 29*:635–642.

Szewczuk Z, Gibbs BF, Yue SY, Purisima E, Zdanov A, Cygler M, Konishi Y. 1993. Design of a linker for trivalent thrombin inhibitors: Interaction of the main chain of the linker with thrombin. *Biochemistry 32*:3396–3404.

Tabernero L, Chang CY, Ohringer SL, Lau WF, Iwanowicz EJ, Han W, Wang TC, Seiler SM, Roberts DGM, Sack JS. 1995. Structure of a retro-binding peptide inhibitor complexed with human α-thrombin. *J Mol Biol 246*:14–20.

Tollefsen DM, Feagler JR, Majerus PW. 1974. The binding of thrombin to the surface of human platelets. *J Biol Chem 249*:2646–2651.

Tronrud D, TenEyck LF, Matthews BW. 1987. An efficient general purpose least squares refinement program for macromolecular structures. *Acta Crystallogr A 34*:489–501.

Tsuda Y, Cygler M, Gibbs BF, Pedyczac A, Féthière J, Yue SY, Konishi Y. 1994. Design of potent bivalent thrombin inhibitors based on hirudin sequence: Incorporation of nonsubstrate-type active site inhibitors. *Biochemistry 33*:14443–14451.

Tulinsky A, Qiu X. 1993. Active site and exosite binding of α-thrombin. *Blood Coagulation and Fibrinolysis 4*:305–312.

van de Locht A, Lamba D, Bauer M, Huber R, Friedrich T, Kröger B, Höffken W, Bode W. 1995. Two heads are better than one: Crystal structure of the insect derived double domain Kazal inhibitor rhodniin in complex with thrombin. *EMBO J 14*:5149–5157.

van de Locht A, Stubbs MT, Bode W, Friedrich T, Bollschweiler C, Höffken W, Huber R. 1996. The ornithodorin–thrombin crystal structure a key to the TAP enigma? *EMBO J 15*:6011–6017.

Vijayalakshmi J, Padmanabhan KP, Mann KG, Tulinsky A. 1994. The isomorphous structure of prethrombin 2 hirugen- and PPACK-thrombin: Changes accompanying activation and exosite binding to thrombin. *Protein Sci 3*:2254–2271.

Vitali J, Martin PD, Malkowski MD, Robertson WD, Lazar JB, Winant RC, Johnson PJ, Edwards BFP. 1992. The structure of a complex of bovine α-thrombin and recombinant hirudin at 2.8 Å resolution. *J Biol Chem 267*:17670–17678.

Vu TKH, Wheaton VI, Hung DT, Charo I, Coughlin SR. 1991. Domains specifying thrombin receptor interaction. *Nature 353*:674–677.

Wu TP, Yee V, Tulinsky A, Chrusciel RA, Nakanashi H, Shen R, Priebe C, Kahn M. 1993. The structure of a designed peptidomimetic inhibitor complex of α-thrombin. *Protein Eng 6*:471–478.

Zdanov A, Wu S, DiMaio J, Konishi Y, Li Y, Wu X, Edwards BFP, Martin PD, Cygler M. 1993. Crystal structure of the complex of human α-thrombin and nonhydrolyzable bifunctional inhibitors hirutonin-2 and hirutonin-6. *Proteins Struct Funct Genet 17*:252–265.